SSRG International Journal of Electronics and Communication Engineering
ISSN: 2348-8549/ https://doi.org/10.14445/23488549/IJECE-V13I11P115

Volume 13 Issue 11, 248-263, November 2026
© 2026 Seventh Sense Research Group®

Original Article

Congestion-Mobility Coupling in AODV-based Mobile Ad Hoc Networks: Traffic Load, False Link Failures and Routing Stability under Three Mobility Models

Rafi U Zaman[1*], Gouri R Patil[1], Sayyada Hajera Begum[2], Gadala Suhasini[2], Padmapriya Patil[3], Fahmina Taranum[4]

[1]*Department of Computer Science and Engineering (Artificial Intelligence), Muffakham Jah College of Engineering and Technology, Telangana, India.*
[2]*Department of Computer Science and Engineering (Artificial Intelligence and Machine Learning), Muffakham Jah College of Engineering and Technology, Telangana, India.*
[3]*Department of Electronics and Communication Engineering, P D A College of Engineering, Kalaburagi, Karnataka, India.*
[4]*Department of Computer Science and Engineering (Data Science), Muffakham Jah College of Engineering and Technology, Telangana, India.*

[*]*Corresponding Author: rafi.u.zaman@mjcollege.ac.in*

Received: 08 October 2026 Revised: 29 October 2026 Accepted: 05 November 2026 Published: 27 November 2026

Abstract *- In reactive routing for Mobile Ad Hoc Networks (MANETs), every link failure reported by the Medium Access Control (MAC) layer is treated as a broken link, although the report may stem from node movement or from congestion. Earlier evaluations vary mobility, node density or traffic load one at a time and count all such reports alike, so the share of route repairs caused by congestion remains unknown. This paper measures how load, density and mobility jointly shape the route stability and service quality of Ad hoc On-Demand Distance Vector (AODV) routing. A full factorial set of 750 ns-2.35 runs combines three mobility models (Random Waypoint, Random Direction and Gauss-Markov), five node counts from 25 to 125 and five per-flow rates from 64 to 128 kb/s. The novelty lies in a paired design, in which each seed fixes the node movement at every rate, and in a geometric test that labels each failure of 45 runs as true or false. In the dense area considered, load explains 69–87 % of the variation in packet delivery ratio, whereas density explains 69–74 % of the variation in normalized routing load. Doubling the rate raises MAC link failures 1.4 to 3.1 times under identical movement, true failures stay unchanged, and 69–84 % of the failures at 128 kb/s are false. Gauss-Markov is the most stable model and Random Direction the least. These results give a baseline for separating congestion from mobility when route repair is evaluated or designed.*

Keywords *- Control overhead, IEEE 802.11 contention, ns-2 simulation, Packet Delivery Ratio, Route repair.*

1. Introduction

Mobile Ad Hoc Networks (MANETs) are formed by wireless nodes which move freely and relay packets for one another, so that neither a base station nor a wired backbone is needed [1, 2]. As each node forwards traffic on behalf of others, the routes are made up of the nodes themselves, and they change whenever the nodes change their positions.

On-demand protocols such as Ad Hoc On-Demand Distance Vector (AODV) routing [3] set up a path just in time, that is, when data is already waiting at a source. This keeps the control traffic small as long as the topology is stable, but it also makes every broken link on an active route expensive: AODV sends a Route Error (RERR), deletes the route and, if packets are still waiting, floods a new Route Request (RREQ) through the network.

A large body of work has examined how node movement affects routing. Comparative simulation studies found that the ranking of routing protocols changes with the mobility of the nodes [4], and surveys of mobility models showed that the speed, the pause time and the correlation between successive movements alter how fast the topology changes [5, 6]. The node density governs connectivity [7], while the traffic load governs how much of the channel capacity is left for control packets [8, 9]. In most of these studies, one of the three factors is changed at a time, and the protocols are judged by delivery ratio, throughput and delay.

An assumption shared by these studies is that a link failure seen by the routing protocol is the result of movement. With IEEE 802.11, however, the MAC layer declares a link broken whenever a frame is not

This is an open access article under the CC BY-NC-ND license (http://creativecommons.org/licenses/by-nc-nd/4.0/)

acknowledged within the retry limit. The next hop may indeed have moved away, but the frame and its retries may equally have been destroyed by collisions, which become more frequent as the load rises [10, 11]. When a routing protocol reacts to such a false failure, it discards a working route, floods a fresh request and buffers or drops the waiting packets, and each of these actions adds to the load that caused the failure in the first place. Movement and congestion are therefore tied together through a single signal, the link failure report, as illustrated in Figure 1.

The research gap addressed in this paper has three parts. Firstly, false link failures have been demonstrated on static topologies or with a single mobility pattern [10-12], but their share has not been measured across mobility models, node densities and loads in one consistent set of experiments. Secondly, performance studies that vary the load or the density [8, 9, 13-15] report end results such as delivery ratio and overhead, but they cannot separate the failures caused by load from those caused by movement, because the movement itself differs from run to run. Thirdly, it is not known whether load and density act on the same performance metrics or on different ones. The problem studied in this paper can therefore be stated as follows: under realistic loads, how much of the route repair performed by AODV is caused by congestion rather than by mobility, and how does this depend on the mobility model and on the node density?

To answer this question, a full factorial campaign of 750 runs is carried out in ns-2.35 [16] with AODV under three mobility models, five node densities and five traffic rates. The novelty of the work lies in two features of its design, neither of which is found in the studies cited above. In the first place, one seeded random number generator drives the movement of the nodes, so that a given seed yields exactly the same movement at every rate; any change in the number of link failures between two rates of the same seed must then be due to the traffic. In the second place, every link failure reported by the MAC layer is labelled true or false by replaying the node positions and testing whether the next hop was still within radio range at the instant of the failure. Together, these two features turn the coupling between congestion and mobility from a plausible explanation into a quantity which can be measured. Two hypotheses, drawn from the literature on mobility models and from preliminary runs, guide the study:

- H1 (congestion-mobility coupling): at light load, the instability due to mobility is largely absorbed, but congestion amplifies it as the traffic rate grows.
- H2 (model sensitivity): owing to the temporal correlation of its movement, the Gauss-Markov model gives more link failures and shorter path stability than the Random Waypoint and Random Direction models.

The main contributions of this paper are as follows:

- A paired design is introduced which keeps the node movement identical while only the traffic load changes, so that failures due to congestion can be told apart from failures due to movement.
- Each MAC link failure is labelled true or false by a geometric test, and the labels show that the true failures do not depend on the load, whereas every extra failure brought by the load is a false one.
- Traffic load and node density are found to govern different metrics: the delivery ratio and the delay follow the load, and the normalized routing load follows the density.
- Hypothesis H1 is confirmed, and hypothesis H2 is reversed: of the three models, Gauss-Markov turns out to be the most stable and Random Direction the least stable.
- The findings are set against those of earlier studies, and the gain in evidence obtained from the paired design, compared with unpaired comparisons, is quantified.

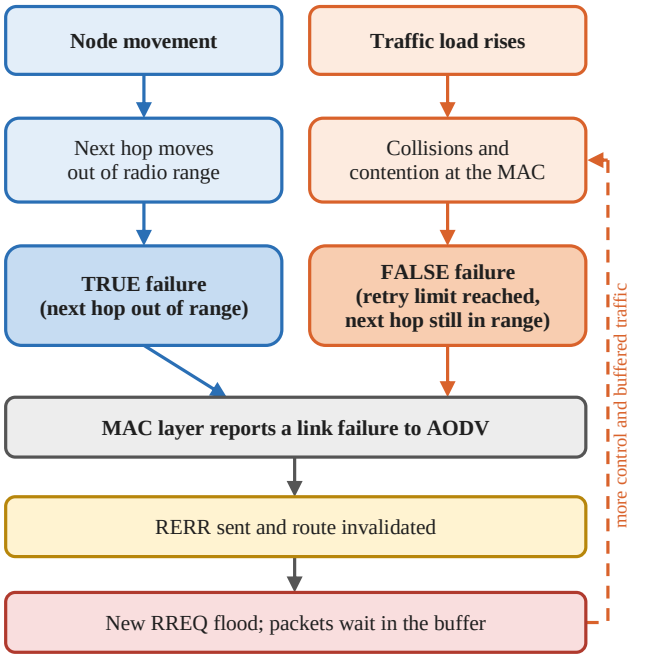

Fig. 1 Coupling between congestion and mobility through the link failure signal in AODV

No new routing protocol is proposed here. The purpose is to quantify false link failures and what they cost, so that protocols designed to avoid them can later be assessed against a firm baseline.

The remaining sections are arranged in the following way. Section 2 reviews the related work and states the research gap. Section 3 describes the simulation set-up, the metrics, the classification of link failures and the statistical analysis. Section 4 presents and discusses the results and compares them with earlier findings. Section 5 concludes the paper.

2. Related Work

2.1. Mobility Models and Routing Performance

Broch et al. [4] evaluated several multi-hop routing protocols in ns-2 and found that their relative standing depends on the mobility of the nodes, which they varied through the pause time of the Random Waypoint model. Camp et al. [5] reviewed the movement patterns that researchers use to evaluate ad hoc networks, including the three models adopted here, and showed that the measured performance of a protocol shifts when a different model is chosen. Yoon et al. [6] pointed out that the average node speed of the Random Waypoint model decreases as a simulation proceeds, which makes averages taken over a run misleading. The Gauss-Markov model was proposed by Liang and Haas [17] for mobility management in personal communication networks. In this model, the speed and direction of a node depend on its previous values, which gives smooth movement that is correlated in time.

2.2. Node Density and Traffic Load

Bettstetter [7] expressed connectivity in terms of the expected number of neighbours per node, a quantity fixed by how densely the nodes are placed and how far they can transmit. Mohapatra and Kanungo [8] used ns-2 to compare AODV, DSR, OLSR and DSDV in terms of delay, throughput, control overhead and packet delivery. Razouqi et al. [9] tested DSDV, DSR and AODV with several patterns of offered traffic and concluded that no single protocol is best in every scenario.

Dubey et al. [13] examined how the load is distributed in AODV and AOMDV as the traffic changes, and Selim et al. [14] assessed eight proactive, reactive and hybrid protocols over a range of node densities. Kour et al. [15] evaluated four protocols in NS-3 for several network sizes and terrain dimensions. These works describe how the performance of the protocols changes with load or density, while the mechanism through which the load alters the behaviour of the routing protocol is outside their scope.

2.3. Link Stability and Stability-Aware Routing

A number of recent schemes build link stability into the routing decision. Pandey and Singh [18] designed a stability-enhanced AODV which prefers routes whose nodes and links satisfy energy and signal-quality thresholds during route discovery. Srilakshmi et al. [19] combined trust-based clustering with an optimization algorithm for selecting routes. Abdellaoui et al. [20] selected the multipoint relays of OLSR by weighing the mobility, the residual energy and the trustworthiness of the candidate nodes. Malarvizhi and Kavithaa [21] identified stable paths with particle swarm optimization and betweenness centrality. Singh et al. [22] applied reinforcement learning to routing in zone-based MANETs, and Abdullah [23] proposed an AODV variant which ranks candidate routes by hop count, remaining battery energy and expected link lifetime in order to cut the number of control packets. All of these schemes estimate the stability of a link from node or link attributes, and they take it for granted that the failures reported to the routing layer are genuine.

2.4. Link Failure Detection under Contention

Xu and Saadawi [10] showed that the 802.11 MAC copes poorly when traffic crosses multiple hops, and that contention between hops can lead a node to report a broken link although its neighbour is still within range. Holland and Vaidya [24] found that route failures severely reduce the throughput of TCP in ad hoc networks, because TCP interprets them as congestion. Li et al. [11] studied false route breakage in 802.11 ad hoc networks, showed that repeated collisions make routing protocols declare working routes broken, and proposed a change to the MAC layer which reduces such events. Valera et al. [12] observed on a real 802.11 testbed that link-layer feedback produces many false detections of link failure, especially at high packet rates. Li et al. [25] showed that the interference between successive hops of a path limits the capacity of an 802.11 multi-hop network, and hence the traffic that it can carry before contention becomes severe.

Table 1. Summary of related work

Ref.	Focus	Mobility	Load changed	Density changed	True/false labelling of failures
[4]	Comparison of routing protocols	RWP (pause time)	No	No	No
[5, 6]	Mobility models and their pitfalls	Several	No	No	No
[7]	Connectivity of ad hoc networks	Analytical	No	Yes	No
[8, 9, 13]	Protocol comparison under load or network size	RWP	Yes	Partly	No
[14, 15]	Protocol assessment across density and terrain	One model	Partly	Yes	No
[18-23]	Stability-aware routing design	One model	Limited	Limited	No
[10-12]	False link failures in 802.11 multi-hop networks	Static or one model	Yes	No	Yes (not across models)
This work	Congestion-mobility coupling in AODV	RWP, RD, GM	Yes (5 rates)	Yes (5 densities)	Yes (geometric test, paired design)

2.5. Summary and Research Gap

The related work is summarised in Table 1. False link failures under contention are well documented [10-12], and their effect on transport protocols is known [24]. These studies, however, use a static topology or a single mobility pattern, and none of them separates, under identical movement, the failures due to mobility from those due to load. The performance studies [8, 9, 13-15] vary the load or the density but treat all link failures alike, and the stability-aware schemes [18-23] rely on these failures being genuine. What is missing is a measurement which holds the movement fixed while the load changes, labels every failure as true or false, and repeats this across mobility models and densities. The present study is designed to provide this measurement.

3. Materials and Methods

3.1. Simulation Environment

The simulations were run in ns-2.35 [16] with the AODV routing protocol [3]. The nodes move inside an area of 600 m × 400 m for 1000 s. The radio channel follows the TwoRayGround propagation model with a 250 m radio range, and the IEEE 802.11 MAC runs with both its data rate and its basic rate set to 1 Mb/s.

Each node has a drop-tail interface queue which holds 50 packets. AODV learns of a broken link from the feedback of the 802.11 MAC layer rather than from periodic HELLO messages, and local repair is disabled. Five Constant Bit Rate (CBR) flows over UDP, with 512-byte packets, link source and destination nodes drawn at random without repetition. The flows start between 20 s and 22 s at intervals of 0.5 s, so that their first route discoveries do not overlap. Table 2 lists the common parameters.

The area is small in relation to the transmission range. Its diagonal of 721 m is spanned by only three hops of full range, so that the paths are short. For nodes placed uniformly in the area, the expected number of neighbours of a node, that is, its degree, is given by

$$\bar{d} = (N - 1)\, p \qquad (1)$$

Where N denotes the count of nodes and p denotes the probability that two uniformly placed nodes lie within the transmission range R of each other. The common approximation $p \approx \pi R^2/A$, with A the area of the region, neglects the effect of the border and gives 0.82, which overstates p because R is comparable with the sides of the region. A numerical evaluation for the 600 m × 400 m area gives $p = 0.49$, that is, an expected degree of about 12 for 25 nodes and about 36 for 75 nodes. Replaying the node positions at 75 nodes gives a measured mean degree of 45.6 for Random Waypoint, 33.4 for Random Direction and 59.5 for Gauss-Markov. Random Direction falls below the uniform value since its nodes spend much of the time near the border, whereas Random Waypoint and Gauss-Markov draw the nodes towards the centre. In every scenario, the degree is far above the level needed for connectivity [7], so that the study is concerned with the stability of routes in a well-connected network and not with partitioning.

3.2. Mobility Models

Three mobility models were used [5]. The speed of every node lies between 1 and 3 m/s, which corresponds to walking pedestrians.

- Random Waypoint (RWP): a target point and a speed are drawn at random for the node; the node walks to that point, stays there for 100 s and then draws a new target.
- Random Direction (RD): a heading and a speed are drawn at random; the node keeps this heading until it touches the border and then draws a new heading without stopping.
- Gauss-Markov (GM): every second, the speed and the direction of a node are updated as a weighted sum of their previous values, their mean values and a Gaussian random term, with memory parameter $\alpha = 0.75$ [17]. The random term has a standard deviation of 0.5 m/s for the speed and $\pi/4$ rad for the direction. When a node enters a border strip whose width is 10 % of each side, its mean direction is turned towards the centre of the area, and a node which is about to leave the area is reflected at the border.

Table 2. Parameters used in the simulations

Parameter	Value
Simulator	ns-2.35 [16]
Routing protocol	AODV [3]
Link failure detection	802.11 link-layer feedback (no HELLO messages), no local repair
Area	600 m × 400 m
Simulation time	1000 s (traffic from 20 s)
Number of nodes	25, 50, 75, 100, 125
Mobility models	RWP (pause 100 s), RD, GM (α = 0.75)
Node speed	1–3 m/s
Traffic	5 CBR flows over UDP, 512-byte packets
Per-flow rate	64, 80, 96, 112, 128 kb/s
MAC	IEEE 802.11, data and basic rate 1 Mb/s
RTS/CTS and retry limits	RTS/CTS on; 7 RTS attempts, 4 data attempts
Propagation	TwoRayGround, range 250 m
Interface queue	Drop-tail, 50 packets
Seeds per configuration	10 (750 runs in total)

All the random choices of a run, including the node movement and the selection of the flows, are taken from one random number generator seeded with the seed of the run. A given seed therefore gives exactly the same movement and

the same flows at every traffic rate. This was checked by running 45 runs of the campaign a second time, which reproduced every metric exactly, and by repeating 20 runs on another computer, which gave identical results.

3.3. Traffic Load and Node Density

The CBR rate of each flow took five values, 64, 80, 96, 112 and 128 kb/s, which give an offered load between 320 and 640 kb/s on a channel whose raw data rate is 1 Mb/s. The number of nodes in the fixed area took the values 25, 50, 75, 100 and 125. Three mobility models, five rates, five densities and ten seeds give a campaign of 750 runs.

3.4. Performance Metrics

Each metric was computed for every run over the traffic period from 20 s to 1000 s, whose length is denoted by T.

- Packet Delivery Ratio (PDR): the share, in per cent, of the data packets generated by the sources that reach their destinations.
- Throughput: the payload bits delivered per second during the traffic period, expressed in kb/s.
- End-to-End Delay: the mean time between the generation of a data packet and its arrival at the destination, taken over all delivered packets.
- Normalized Routing Load (NRL): the number of routing control transmissions (RREQ, RREP and RERR, with every retransmission counted) divided by the number of data packets delivered.
- Link Breakage Rate (LBR): the number of link failures per second which the MAC layer reports to AODV, where repeated reports for one link within one second are counted once.
- Path Stability Time (PST): the mean duration of the intervals during which a flow is delivered without a break, an interval being closed when more than one second passes between two received packets.

The LBR and the PST are given by

$$LBR = \frac{F}{T} \tag{2}$$

$$PST = \frac{1}{N_p}\sum_{k=1}^{N_p} \tau_k \tag{3}$$

Here F counts the MAC link failures of the run after duplicates are removed, N_p counts the delivery intervals completed by all flows, and τ_k is the duration of the k-th interval. Intervals that have not closed when the simulation stops are treated as censored and excluded from Equation 3.

With a fixed run length, the LBR is simply proportional to the number of failures in a run, so the results that follow are stated as failures per run.

3.5. Classification of Link Failures

In the simulator, AODV is told of a failure by the MAC layer once seven RTS attempts or four data attempts have gone unanswered. An attempt fails in exactly the same way whether the next hop has left the range or an RTS, CTS, data or acknowledgement frame has collided. Each failure reported at time t on the link from node i to its next hop j is therefore labelled according to

$$\text{failure} = \begin{cases} \text{true}, & d_{ij}(t) > R \\ \text{false}, & d_{ij}(t) \le R \end{cases} \tag{4}$$

Here, $d_{ij}(t)$ is the separation of the two nodes at time t, found by replaying the recorded movement, and R = 250 m is the radio range. A true failure is one where the next hop had genuinely moved beyond reach; in a false failure, it was still within reach, and the frame was destroyed by collisions or contention. Labels were produced for 45 runs, covering the three mobility models and the five rates at 75 nodes with seeds 1, 2 and 3. These runs are part of the main campaign; they were run again with the next hop of every failure recorded. The steps are listed below.

Algorithm for Classifying MAC Link Failures as True or False

//1. Record the failures during the simulation

Step 1: Whenever the routing layer drops a packet with reason CBK (callback from the MAC layer), log the time t, the node i and the next hop's MAC address j.

Step 2: If a failure of the same link (i, j) was already stored within the last second, discard the record; otherwise, count it as one link failure.

//2. Replay the node movement

Step 3: Read the movement commands of all nodes from the scenario file and obtain the position of every node at any time by linear interpolation along its current movement.

//3. Classify each failure

Step 4: For each logged failure (t, i, j), find the distance $d_{ij}(t)$ separating i from j at time t.

Step 5: If $d_{ij}(t) > R$, label the failure as true, since the next hop is outside the radio range.
Otherwise, label it as false, since the next hop was still in range and the frame was lost to collisions or contention.

Step 6: Count the true and false failures of the run; the false share is the ratio of false failures to all failures.

3.6. Experimental Design and Statistical Analysis

All values are given as means over ten seeds, together with a 95 % confidence interval from the t-distribution. The influence of the load on link failures is assessed on paired runs. For each mobility model, the 50 pairs of runs at 64 and 128 kb/s with equal density and seed share the same

movement, and their within-pair differences are examined with the Wilcoxon signed-rank test.

To weigh load against density, the part of the total variation of a metric that the factor-level means account for is calculated once for the rate and once for the node count. The way the routing load scales with density is captured by the fit

$$\log NRL = k \log N + c \quad (5)$$

Here k is the density exponent, and c is a constant, which means the routing load scales as N^k. A 95 % confidence interval for k is obtained from 2000 bootstrap resamples of the seeds.

4. Results and Discussion

4.1. Packet Delivery and Saturation

Figure 2 presents the packet delivery ratio, and Table 3 gives its values pooled over the five densities. Under every mobility model and at every density, delivery worsens steadily as the rate rises. With 64 kb/s flows, the ratio is 97.3 % for Random Waypoint, 98.7 % for Gauss-Markov and 90.2 % for Random Direction; with 128 kb/s flows, it drops to 68.6 %, 79.0%, and 52.5 %, respectively.

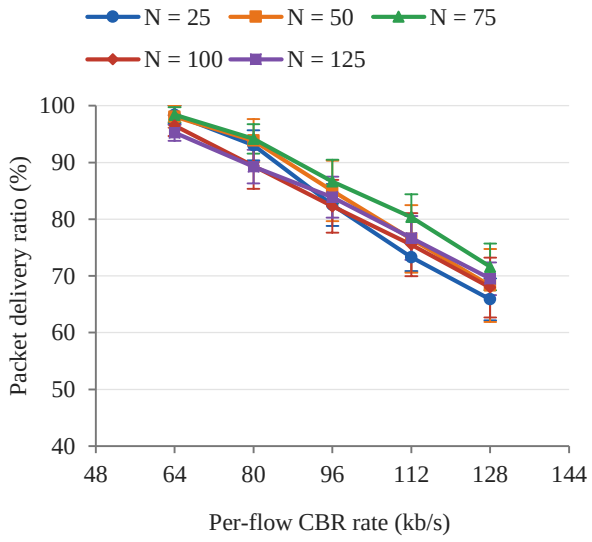

(a) Random Waypoint

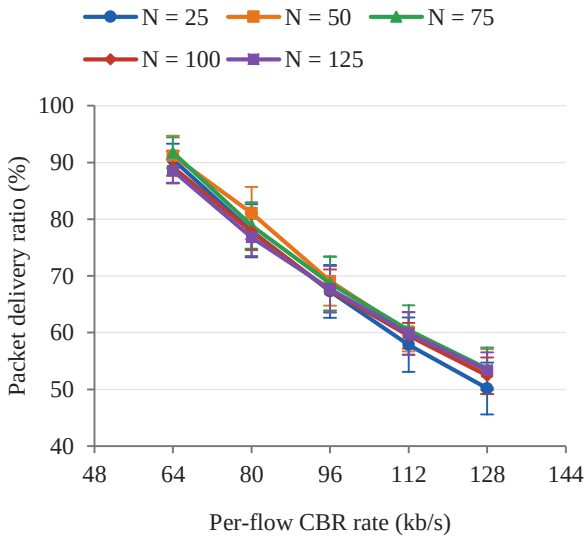

(b) Random Direction

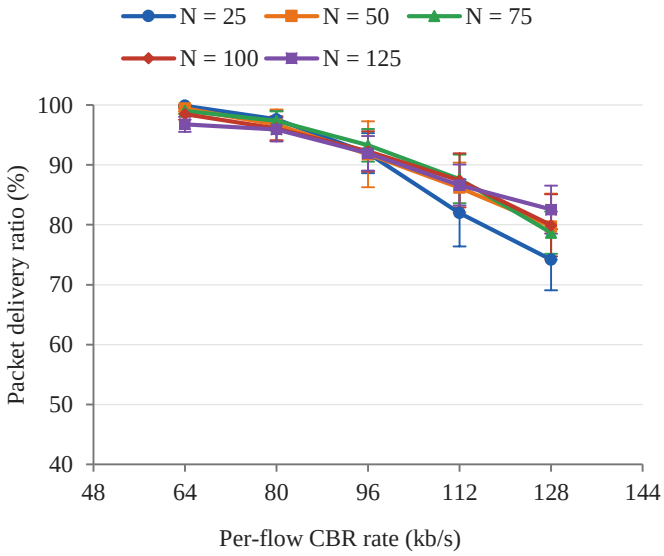

(c) Gauss-Markov

Fig. 2 Packet delivery ratio versus per-flow CBR rate: (a) Random Waypoint, (b) Random Direction, and (c) Gauss-Markov (Mean of 10 seeds; bars show the 95 % confidence interval).

Table 3. Results pooled over the five densities (Mean ± 95 % confidence interval, 50 runs per cell)

Model	CBR rate (kb/s)	Delivery ratio (%)	Mean delay (s)	Throughput (kb/s)	Link failures in a run	Path stability (s)
RWP	64	97.3 ± 0.7	0.12 ± 0.04	311 ± 2	57 ± 13	185 ± 37
RWP	96	84.1 ± 1.7	0.82 ± 0.11	403 ± 8	93 ± 17	45 ± 7
RWP	128	68.6 ± 1.9	1.42 ± 0.12	439 ± 12	105 ± 14	25 ± 3
RD	64	90.2 ± 1.1	0.42 ± 0.06	288 ± 4	317 ± 52	49 ± 27
RD	96	68.0 ± 1.7	1.55 ± 0.10	326 ± 8	426 ± 70	15 ± 1
RD	128	52.5 ± 1.5	2.06 ± 0.10	336 ± 9	429 ± 65	13 ± 1
GM	64	98.7 ± 0.4	0.04 ± 0.02	316 ± 1	21 ± 3	176 ± 47
GM	96	92.2 ± 1.4	0.40 ± 0.09	442 ± 7	40 ± 6	96 ± 23
GM	128	79.0 ± 2.0	1.00 ± 0.10	505 ± 13	65 ± 9	34 ± 3

A convenient marker of where the decline starts is the lowest rate at which the mean delivery ratio drops under 95 %. At every density, this marker lies at 80 kb/s for Random Waypoint and at 96 kb/s for Gauss-Markov, whereas Random Direction is under 95 % from 64 kb/s onwards. Since the fall is gradual, with no abrupt switch between separate operating phases, such a threshold describes it better than a division into phases.

In Figure 2, the curves of the five densities nearly coincide. Under Random Waypoint, the delivery ratio spans only 95.2–98.4 % across densities at 64 kb/s and 65.9–71.6 % at 128 kb/s. The rate accounts for 78 % (RWP), 87 % (RD) and 69 % (GM) of the total variation in the delivery ratio, against at most 2 % for the node count. Thus, it can be said that, over the range studied, the delivery level is set by the traffic load and not by the node density.The individual runs show the same picture. At 64 kb/s, single runs deliver between 91.3 % and 99.9 % of the packets under Random Waypoint and between 94.1 % and 100.0 % under Gauss-Markov, and only 10 and 3 of the 50 runs, respectively, stay below 95 %. Under Random Direction, 45 of the 50 runs are already below this level, and 24 are below 90 %, with values as low as 81.9 %. At 128 kb/s, no run of any model reaches 95 %: single runs range from 47.1 % to 80.2 % under Random Waypoint, from 41.4 % to 63.3 % under Random Direction and from 64.0 % to 92.1 % under Gauss-Markov. The spread between seeds also widens with the load. The standard deviation of the delivery ratio over the ten seeds of a configuration, averaged over the densities, grows from 2.3 to 6.3 percentage points for Random Waypoint and from 0.9 to 6.5 for Gauss-Markov between 64 and 128 kb/s, and it is 3.9 and 5.2 for Random Direction. Within each rate, runs with more MAC link failures deliver fewer packets (mean correlation between −0.40 and −0.57), which anticipates the role of the link failures examined in Sections 4.4 and 4.5. The delivery ratio is also strongly and negatively correlated with the delay (−0.72 to −0.82), so that the runs which lose more packets also deliver the remaining ones later.

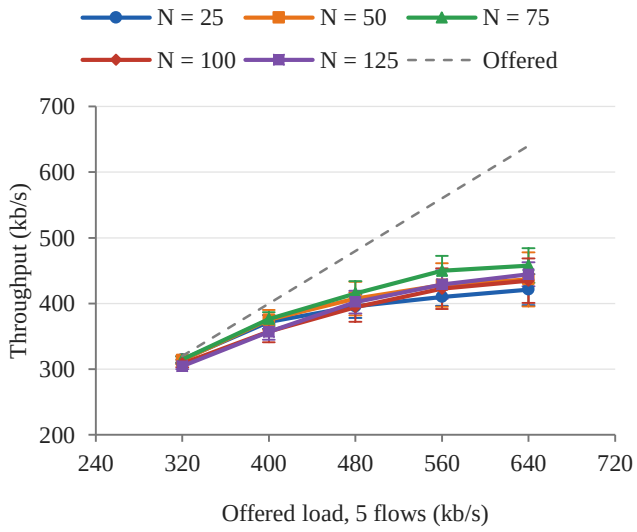

(a) Random WayPoint

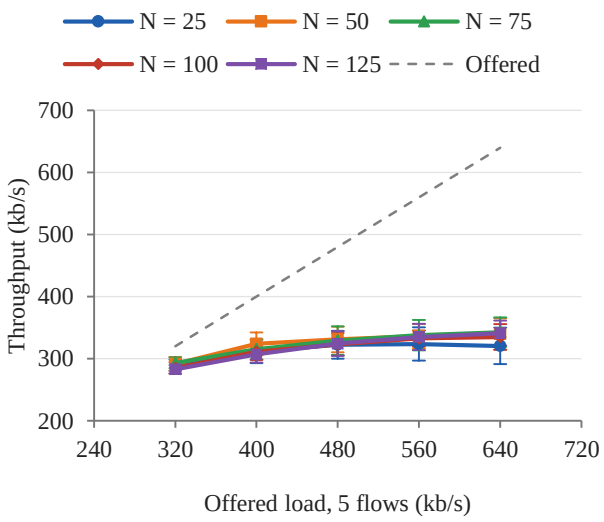

(b) Random Direction

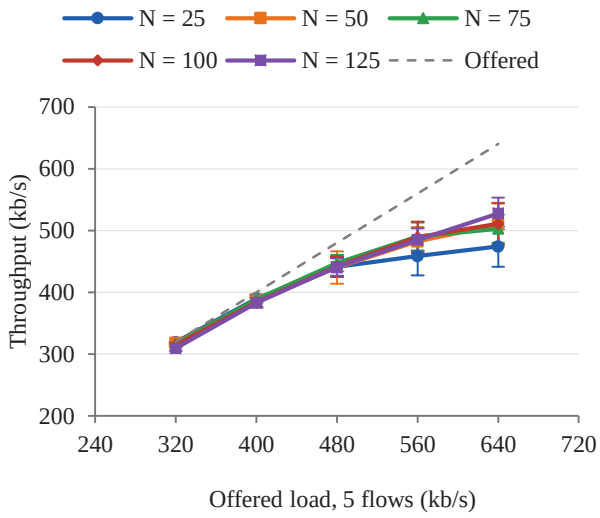

(c) Gauss-Markov

Fig. 3 Throughput versus offered load: (a) Random Waypoint, (b) Random Direction, and (c) Gauss-Markov (Mean of 10 seeds; bars show the 95 % confidence interval; dashed line: throughput equal to offered load).

The reason for this decline is visible in Figure 3, where throughput is plotted against the offered load. Until the offered load reaches 400 kb/s, Gauss-Markov delivers almost all of it and Random Waypoint falls short by no more than about 10 %. At higher loads, the curves flatten: with 640 kb/s offered, Random Waypoint carries 421–458 kb/s and Gauss-Markov 474–528 kb/s, depending on the density, and Random Direction never carries more than 343 kb/s. Saturation thus sets in far below the 1 Mb/s channel rate, which agrees with the capacity bound that interference between consecutive hops of a path imposes on 802.11 multi-hop networks [25].

4.2. End-to-End Delay

Figure 4 plots the end-to-end delay. With 64 kb/s flows, packets take 0.04 s on average under Gauss-Markov, 0.12 s under Random Waypoint and 0.42 s under Random Direction; with 128 kb/s flows, the averages grow to 1.00 s, 1.42 s and 2.06 s, which is 5 to 25 times longer.

Close to saturation, packets spend time in the interface queues, and those whose route has just failed are parked in the routing buffer until a new route is found. The density again matters little for the delay in comparison with the rate.

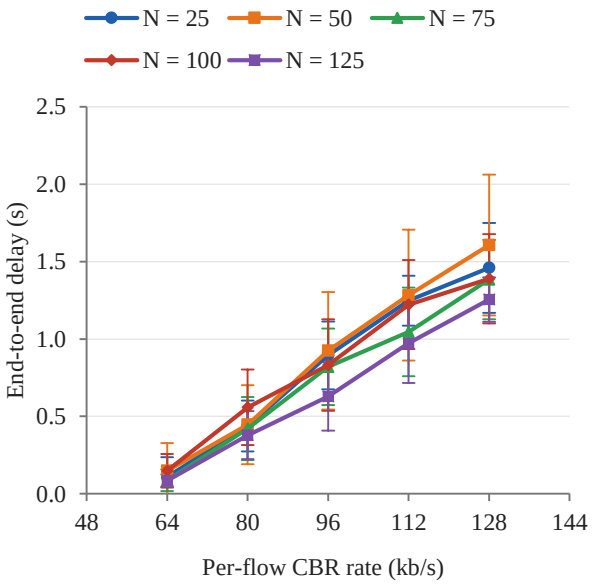

(a) Random Waypoint

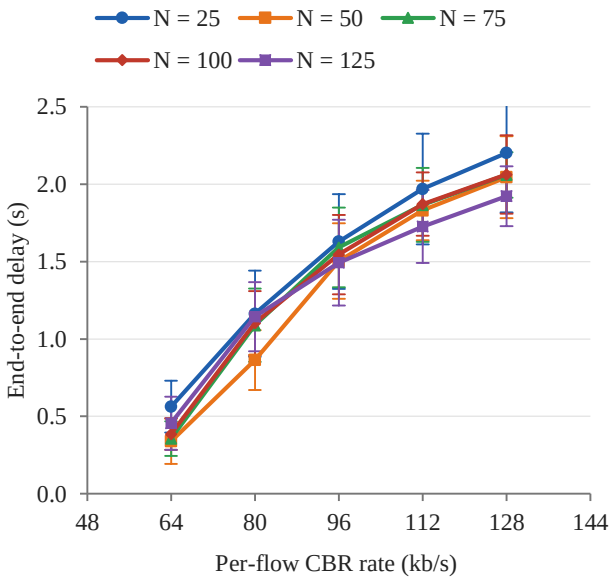

(b) Random Direction

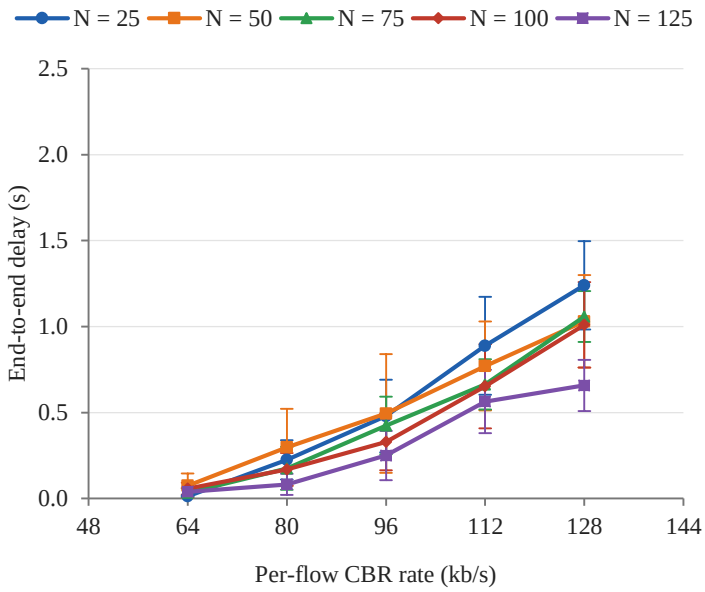

(c) Gauss-Markov

Fig. 4 End-to-end delay versus per-flow CBR rate: (a) Random Waypoint, (b) Random Direction, and (c) Gauss-Markov (Mean of 10 seeds; bars show the 95 % confidence interval).

4.3. Routing Overhead and Node Density

Figure 5 presents the normalized routing load on a logarithmic scale. In contrast with the delivery ratio, it is driven by the node count and hardly by the rate. At 64 kb/s, going from 25 to 125 nodes raises it from 0.033 to 0.215 under Random Waypoint, from 0.130 to 0.704 under Random Direction and from 0.010 to 0.128 under Gauss-Markov. The node count accounts for 69–74 % of the variation in the logarithm of the routing load, while the rate accounts for no more than 2 %. The explanation lies in what the control traffic consists of. Between 96 and 98 % of the control packets are route requests, and since every node that hears a request rebroadcasts it, one route discovery costs more as the node count grows. The density exponents of Equation 5 (Table 4) range from 1.05 to 1.56 at 64 kb/s, indicating that the routing load grows faster than in proportion to the number of nodes. At 128 kb/s, the three models converge to exponents of 1.18 to 1.23.

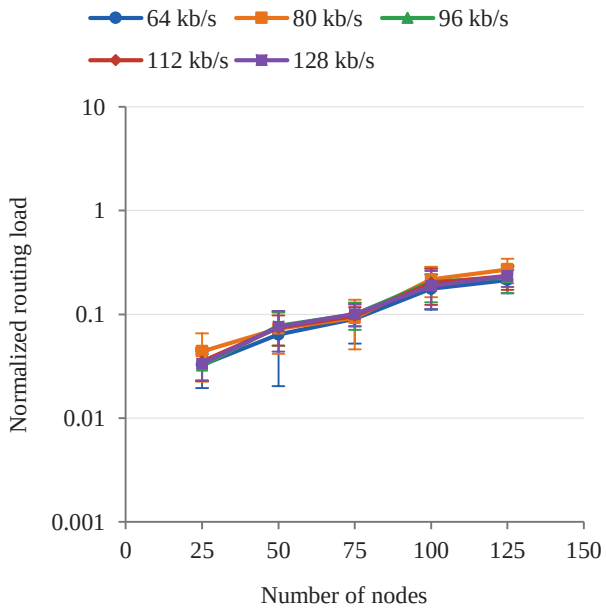

(a) Random Waypoint

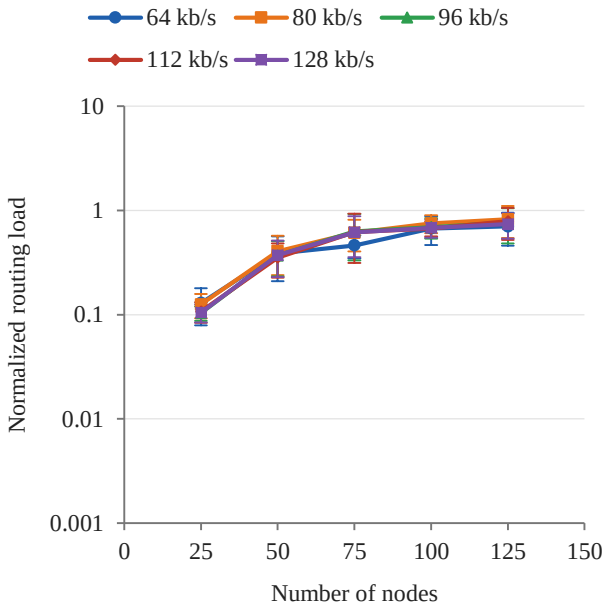

(b) Random Direction

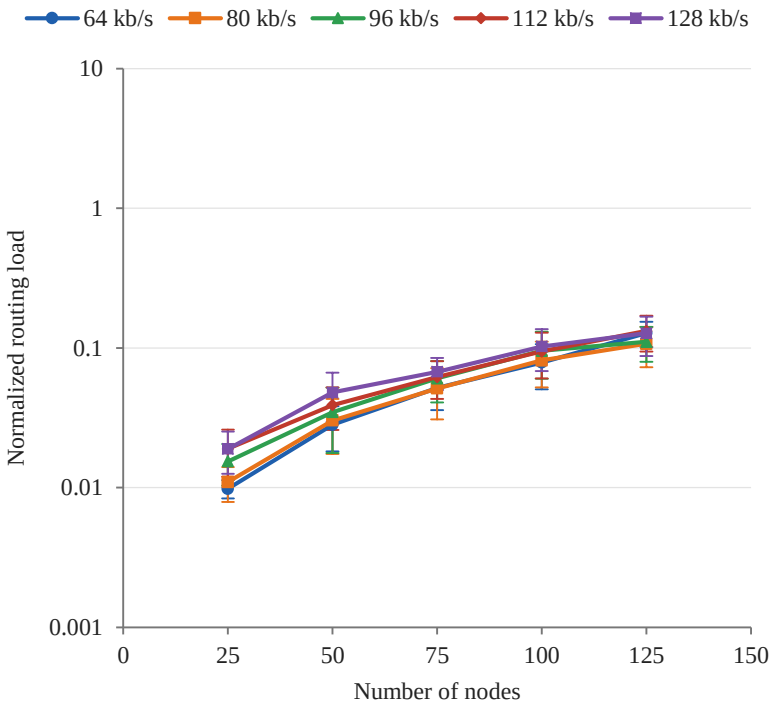

(c) Gauss-Markov

Fig. 5 Normalized routing load versus number of nodes, logarithmic scale: (a) Random Waypoint, (b) Random Direction, and (c) Gauss-MARKOV (Mean of 10 seeds; bars show the 95 % confidence interval).

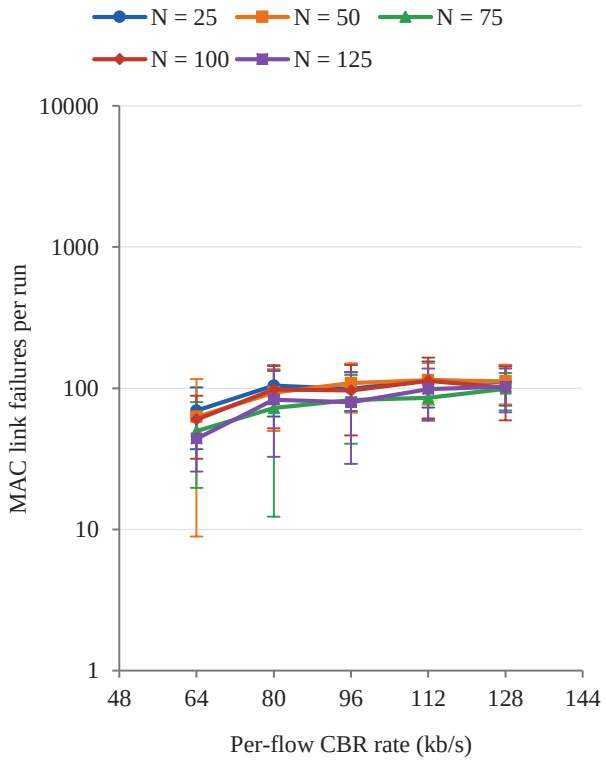

(a) Random Waypoint

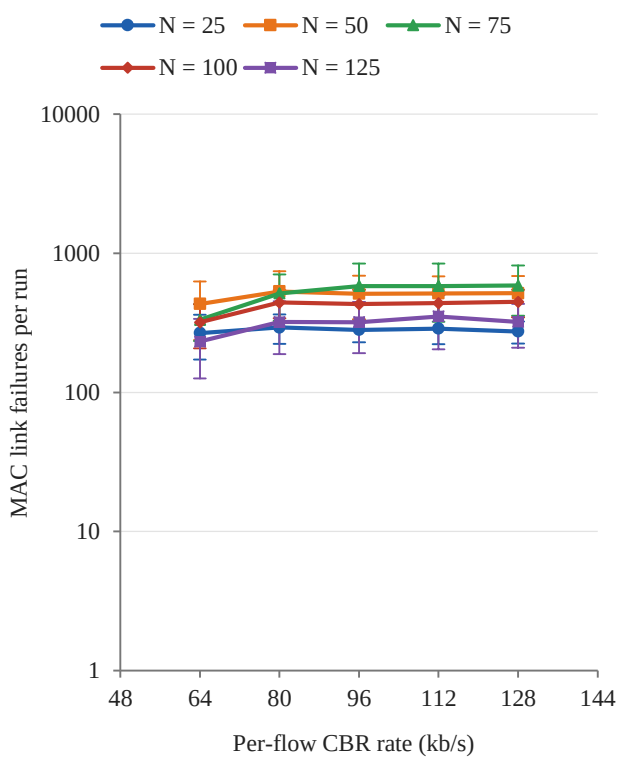

(b) Random Direction

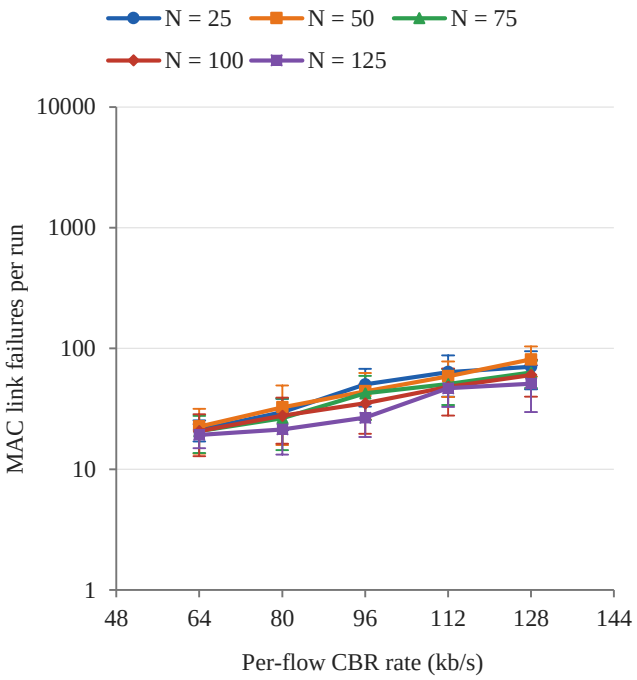

(c) Gauss-Markov

Fig. 6 MAC link failures per run versus per-flow CBR rate, logarithmic scale: (a) Random Waypoint, (b) Random Direction, and (c) Gauss-Markov (mean of 10 seeds; bars show the 95 % confidence interval).

It may be noted that the normalized routing load masks the influence of the load. The control packets sent per run do grow with the rate: between 64 and 128 kb/s they rise 1.53-fold under Random Waypoint, 1.97-fold under Gauss-Markov and 1.24-fold under Random Direction, with the movement held fixed. As more data packets are also delivered at higher rates, the ratio barely moves. The next subsection traces where the extra control packets come from.

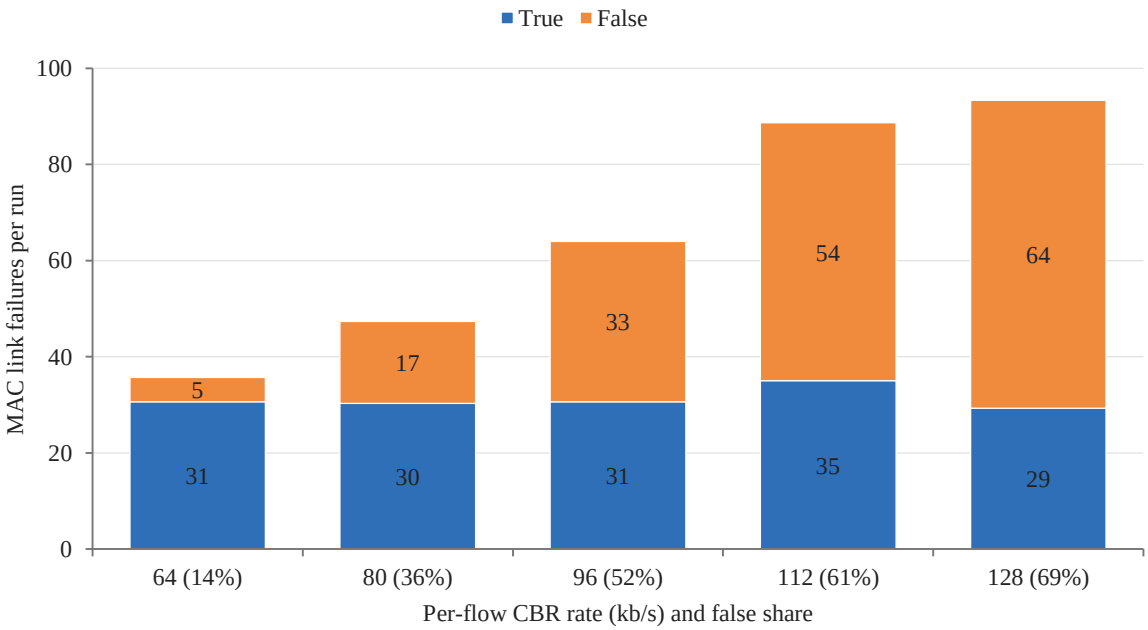

(a) Random Waypoint

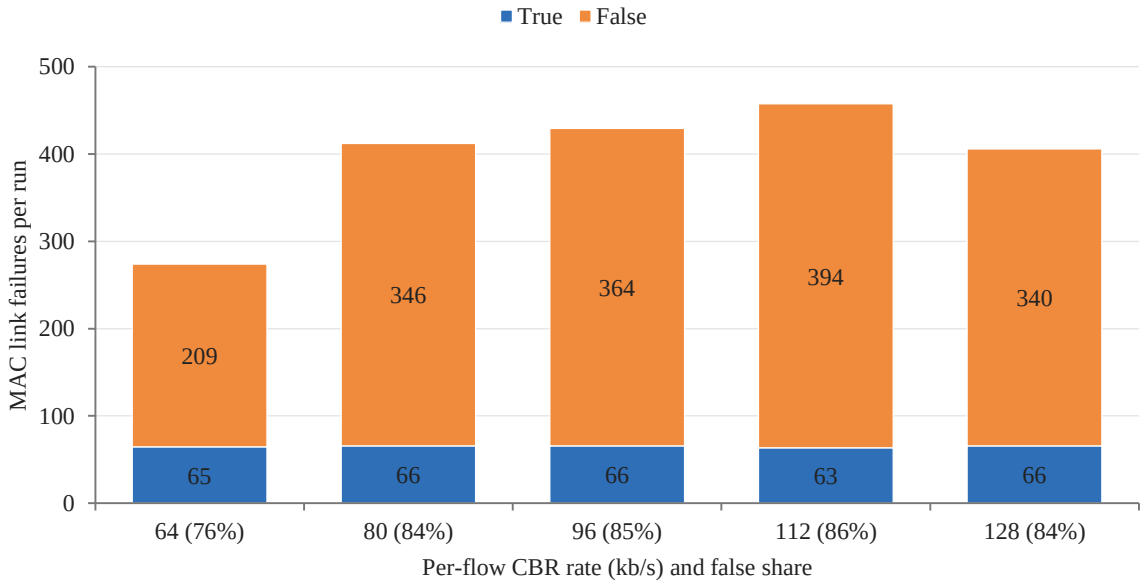

(b) Random Direction

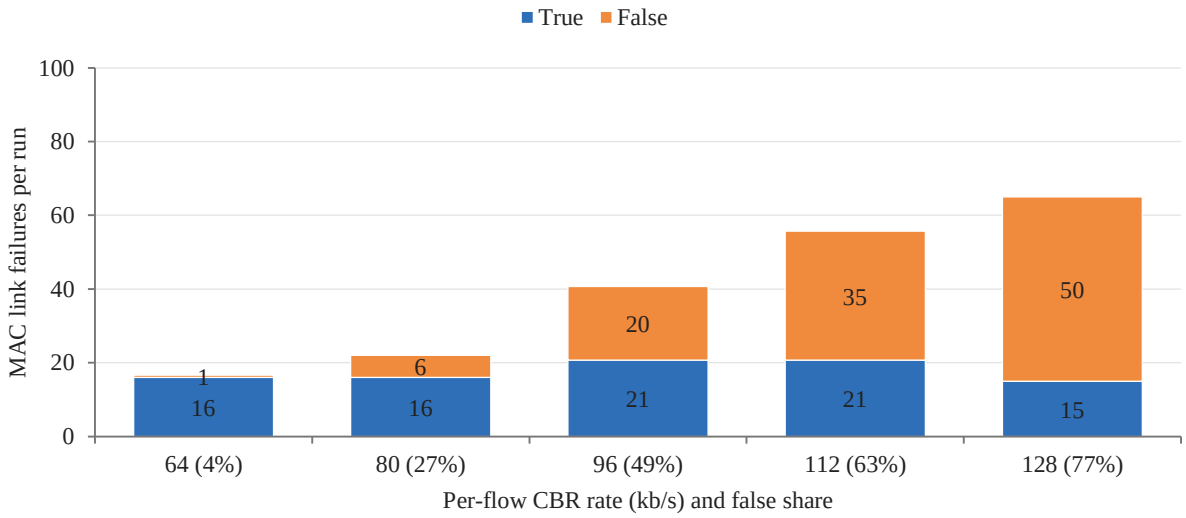

(c) Gauss-Markov

Fig. 7 True and false MAC link failures per run at 75 nodes (mean of seeds 1–3): (a) Random Waypoint, (b) Random Direction, and (c) Gauss-Markov; the false share is given below each rate.

Table 4. Density exponent k of the normalized routing load (Equation 5), with 95 % bootstrap interval

Model	Exponent k, 64 kb/s	Fit R^2	Exponent k, 128 kb/s	Fit R^2
RWP	1.19 [1.02, 1.38]	0.97	1.20 [1.08, 1.34]	0.98
RD	1.05 [0.93, 1.20]	0.95	1.23 [1.15, 1.32]	0.93
GM	1.56 [1.42, 1.67]	1.00	1.18 [1.02, 1.33]	0.99

4.4. Congestion-Induced Link Failures

Figure 6 gives the count of link failures that the MAC layer passes to AODV. Because a given density and seed produce the same movement at all rates, every rise along a curve in Figure 6 must come from the traffic. The count goes up with the rate under all three models. Table 5 sets the 50 run pairs at 64 and 128 kb/s side by side for each model: the failures grow by 47.8 per run under Random Waypoint (in 48 of 50 pairs), by 44.3 under Gauss-Markov (in every pair) and by 112.8 under Random Direction (in 42 of 50 pairs). The Wilcoxon signed-rank test finds all three increases significant ($p < 10^{-5}$).

Table 5. MAC link failures at 64 and 128 kb/s with identical node movement (50 pairs per model)

Model	Mean failures, 64 kb/s	Mean failures, 128 kb/s	Mean change within pairs (95 % CI)	Pairs with more failures at 128 kb/s	Failure ratio	Control packet ratio	p (Wilcoxon)
RWP	57.1	105.0	+47.8 ± 10.6	48/50	1.84	1.53	1.0×10^{-8}
RD	316.7	429.4	+112.8 ± 44.5	42/50	1.36	1.24	1.1×10^{-6}
GM	20.9	65.2	+44.3 ± 7.2	50/50	3.12	1.97	7.5×10^{-10}

Thus, it can be said that congestion generates link failures that AODV has no means of distinguishing from those due to movement. Every such failure on a data packet triggers a RERR and removes the route, and when the source still has data to send, a fresh flood of route requests follows. This accounts, at least partly, for the rise in control packets noted in Section 4.3. It is precisely the coupling of congestion and mobility stated in hypothesis H1, measured directly by the paired design.

4.5. True and False Link Failures

Which of these failures reflect real breaks is revealed by the labelling of Section 3.5, summarised in Figure 7 and Table 6. Under Random Waypoint, the true failures lie between 29 and 35 per run whatever the rate, whereas the false failures climb from 5 at 64 kb/s to 64 at 128 kb/s, lifting the false share from 14 % to 69 %. The same pattern appears for Gauss-Markov, with 15–21 true failures per run and a false share rising from 4 % to 77 %. Random Direction keeps 63–66 true failures per run as well, but its false share is 76 % even at 64 kb/s and 84–86 % at the higher rates.

These labels confirm the mechanism. With the movement unchanged, the true failures stay level as the load rises, as they should, and all of the extra failures are false ones whose next hop was still within range. At 128 kb/s, therefore, roughly two-thirds to five-sixths of the failures that trigger AODV route repair involve links that were intact. False route breakage is a known effect [10-12]; what the present results add is its size across mobility models and loads, and the observation that under heavy load it outweighs the effect of mobility.

It is also worth noting how rarely a geometric link change touches the routing. Replaying the positions shows that, in a run at 75 nodes, about 4,750 (RWP), 5,500 (RD) and 5,760 (GM) node pairs lose radio contact, yet on average only 15 to 66 failures per run involve a link that carries traffic at that instant.

4.6. Comparison of the Mobility Models

The results contradict hypothesis H2, which predicted that Gauss-Markov would be the least stable model. Of the three models, Gauss-Markov records the smallest number of true link failures (15–21 per run) together with the best delivery ratio, the shortest delay and the smallest routing load. The weakest model is Random Direction, with 63–66 true failures per run (three to four times the Gauss-Markov figure), a delivery ratio of just 90.2 % already at 64 kb/s, and a routing load between three and six times that of Random Waypoint.

Table 6. True and false MAC link failures in a run (75 nodes, seeds 1–3; False % = share of false failures)

CBR rate (kb/s)	True, RWP	False, RWP	False %, RWP	True, RD	False, RD	False %, RD	True, GM	False, GM	False %, GM
64	30.7	5.0	14 %	64.7	209.3	76 %	16.0	0.7	4 %
80	30.3	17.0	36 %	65.7	346.3	84 %	16.0	6.0	27 %
96	30.7	33.3	52 %	65.7	363.7	85 %	20.7	20.0	49 %
112	35.0	53.7	61 %	63.3	394.0	86 %	20.7	35.0	63 %
128	29.3	64.0	69 %	65.7	340.0	84 %	15.0	50.0	77 %

Why the models differ becomes clear from how each of them spreads the nodes over the area and moves them. Under Random Direction, a node keeps its heading until it reaches the border, so a large fraction of the nodes is found close to the edges at any moment. At 75 nodes, the measured mean degree is therefore only 33.4, lower than the figure of about 36 predicted for a uniform layout; paths become longer, and more of the links in use are close to the edge of the radio range. Gauss-Markov changes speed and heading gradually and turns nodes near the border back towards the middle, so the nodes crowd in the central part of the area. Its mean degree rises to 59.5, and since most neighbours are well inside the range, few links come near breaking. Random Waypoint keeps each node still for 100 s after every trip, which puts it between the other two models. This reading is supported by the measured degrees but was not isolated in a separate experiment; it also means that the comparison of models combines two effects, the time correlation of the movement and the spatial spread of the nodes.

Table 7. Comparison of the present findings with those of earlier studies

Ref.	Setting of the earlier study	Earlier finding	Finding of the present study
[4]	ns-2, RWP with varied pause time, fixed load	Protocol performance depends on node mobility	Under identical movement, raising the load multiplies MAC link failures by 1.4–3.1, so load and mobility must be studied together
[5]	Survey of mobility models	Measured performance changes with the mobility model	Confirmed; GM is the most stable and RD the least, which is traced to the spatial distribution of the nodes
[9]	DSDV, DSR and AODV under several traffic load patterns	The best protocol depends on the traffic pattern	For AODV, the load explains 69–87 % of the variation in PDR, the density at most 2 %
[14]	Eight protocols over a range of node densities	Performance changes with node density	The density explains 69–74 % of the variation in NRL, which grows as $N^{1.05}$ to $N^{1.56}$
[10, 11]	Static 802.11 multi-hop topologies	Collisions cause false link breakage	False share of 69–84 % at 128 kb/s under all three mobility models, with true failures unchanged by the load
[12]	Real 802.11 testbed	Many false detections of link failure at high packet rates	False share rises from 4–14 % (GM, RWP) at 64 kb/s to 69–77 % at 128 kb/s
[25]	Analysis and simulation of 802.11 chains	Capacity limited by interference between hops	Throughput saturates at 421–528 kb/s for 640 kb/s offered, well below 1 Mb/s

4.7. Path Stability Time

Table 3 shows that the path stability time shrinks as the rate is raised from 64 to 128 kb/s: from 185 s to 25 s under Random Waypoint, from 176 s to 34 s under Gauss-Markov and from 49 s to 13 s under Random Direction. Equation 3 closes a delivery interval as soon as a flow is silent for longer than one second, irrespective of whether the silence comes from a failed route or from packets lost in a full queue. Near saturation, queue losses prevail, so the metric then reflects how continuously packets are delivered rather than how long routes survive, and it is best interpreted alongside the failure counts of Sections 4.4 and 4.5.

4.8. Comparison with Existing Studies

Table 7 compares the main findings of this study with those reported in the related literature. Where the settings overlap, the present results agree with the earlier ones: the performance of AODV depends on the mobility model [4, 5], the network saturates well below the raw data rate [25], and contention produces false link failures [10-12]. The present study extends these findings in three respects. Firstly, the share of false failures is measured under three mobility models and five loads instead of a single pattern, and it is shown to reach 69–84 % at 128 kb/s in all three.

Secondly, the true failures are shown to remain constant as the load grows, which identifies every additional failure as an effect of congestion. Thirdly, the roles of the two scale factors are separated: the load sets the delivery ratio and the delay, whereas the density sets the routing load, a distinction which studies varying one factor at a time [9, 14] could not draw.

4.9. Why the Paired Design Gives Clearer Evidence

The study does not propose a new protocol, and its results are not claimed to outperform existing schemes. Its advantage lies in the strength of the evidence which it provides on the cause of route repair, and three features of the method account for this. Firstly, the paired seeds remove the variation due to movement. The failure counts of two runs with the same seed and density at 64 and 128 kb/s are strongly correlated ($r = 0.63–0.73$), so that the movement alone explains about 40–53 % of their variation. For Random Direction, where this variation is largest, an unpaired comparison of the same 100 runs gives $p = 3.2 \times 10^{-3}$ (Mann-Whitney test), whereas the paired test gives $p = 1.1 \times 10^{-6}$. A study that compares different movements at the two rates would therefore need many more runs to detect the same effect. Secondly, the geometric test gives a ground truth which testbed studies cannot obtain, since the exact position of every node is known at every instant; on a real testbed, false detections can be observed only indirectly [12], whereas here every failure of the 45 classified runs carries a label. Thirdly, the full factorial design attributes the variation of each metric to the load or to the density, which is not possible when one factor is varied at a time [4, 9, 14].

4.10. Implications

Two consequences follow for the way routing protocols in MANETs are evaluated and designed. First, when the network carries a significant load, the count of link failures reported by the MAC layer no longer measures mobility. Work that uses link breakage rates to rank mobility models, or to tune stability-aware routing, should therefore either stay

below the saturation point or separate true failures from false ones. Second, a reactive protocol that repairs a route after a false failure adds to the very congestion that produced it. Most of the repairs seen at high load could be avoided by a repair scheme that first checks whether the next hop still answers, or that takes the local channel load into account before a route is dropped.

4.11. Scope and Limitations

Some limitations of the work should be noted. AODV is the only protocol examined, and proactive protocols, which respond differently to single link failures, may not show the same pattern. The true/false labelling rests on 45 runs at one density with three seeds, even though its outcome is consistent over every rate and model. Because the TwoRayGround model gives a sharp edge to the radio range, the geometric labelling is exact in simulation, while real channels fade gradually. Node speeds are kept at walking pace, and the area is small enough that any two nodes are only a few hops apart. Lastly, all traffic is carried by five CBR flows over UDP; with an adaptive source such as TCP, the losses would feed back into the offered load.

5. Conclusion

Routing in mobile ad hoc networks rests on how well broken links are detected, and reactive protocols such as AODV accept every failure signalled by the MAC layer as a real break. This paper quantified how traffic load, node density and mobility together influence AODV, using a paired campaign of 750 simulation runs under three mobility models, and labelled the link failures of 45 of these runs as true or false.

Within the dense area considered, the level of delivery is fixed by the traffic load and not by the number of nodes. Moving from 64 to 128 kb/s per flow, the delivery ratio drops from 90–99 % to 53–79 %, and the delay grows five- to twenty-five-fold, while a higher node count mostly adds to the normalized routing load. For the same movement, the heavier load multiplies the MAC link failures by 1.4 to 3.1 but leaves the true failures unchanged, so that 69–84 % of the failures labelled at 128 kb/s are false. Hypothesis H1 is thus supported and quantified, whereas hypothesis H2 is reversed, with Gauss-Markov emerging as the most stable model and Random Direction as the least stable.

Future work will apply the true/false labelling to every density and seed of the campaign and to proactive protocols, DSDV in particular. A route repair scheme for AODV that verifies the next hop is really unreachable before dropping a route will also be evaluated. A further open question is how the coupling behaves at higher node speeds and with TCP traffic.

Data Availability Statement

The per-run results which support the findings of this study are available from the corresponding author on reasonable request.

Conflicts of Interest

The authors declare that there is no conflict of interest regarding the publication of this paper.

Funding Statement

The authors received no funding for this work.

References

[1] S. Corson, and J. Macker, “Mobile Ad Hoc Networking (MANET): Routing Protocol Performance Issues and Evaluation Considerations,” *IETF RFC 2501*, 1999. [Google Scholar] [Publisher Link]

[2] Charles E. Perkins, *Ad Hoc Networking*, Addison-Wesley, pp. 1-28, 2008. [Google Scholar] [Publisher Link]

[3] C. Perkins, E. Belding-Royer, and S. Das, “Ad Hoc On-Demand Distance Vector (AODV) Routing,” *IETF RFC 3561*, 2003. [Google Scholar] [Publisher Link]

[4] Josh Broch et al., “A Performance Comparison of Multi-Hop Wireless Ad Hoc Network Routing Protocols,” *Proceedings of the 4th Annual ACM/IEEE International Conference on Mobile Computing and Networking (MobiCom)*, Association for Computing Machinery, New York, United States, pp. 85-97, 1998. [CrossRef] [Google Scholar] [Publisher Link]

[5] Tracy Camp, Jeff Boleng, and Vanessa Davies, “A Survey of Mobility Models for Ad Hoc Network Research,” *Wireless Communications and Mobile Computing*, vol. 2, no. 5, pp. 483-502, 2002. [CrossRef] [Google Scholar] [Publisher Link]

[6] J. Yoon, Mingyan Liu, and Brian Noble, “Random Waypoint Considered Harmful,” *IEEE INFOCOM 2003. Twenty-second Annual Joint Conference of the IEEE Computer and Communications Societies (IEEE Cat. No.03CH37428)*, Francisco, CA, USA, pp. 1312-1321, 2003. [CrossRef] [Google Scholar] [Publisher Link]

[7] Christian Bettstetter, “On the Connectivity of *Ad Hoc* Networks,” *The Computer Journal*, vol. 47, no. 4, pp. 432-447, 2004. [CrossRef] [Google Scholar] [Publisher Link]

[8] S. Mohapatra, and P. Kanungo, “Performance Analysis of AODV, DSR, OLSR and DSDV Routing Protocols using NS2 Simulator,” *Procedia Engineering*, vol. 30, pp. 69-76, 2012. [CrossRef] [Google Scholar] [Publisher Link]

[9] Qutaiba Razouqi et al., “Extended Comparison and Performance Analysis for Mobile Ad-Hoc Networks Routing Protocols based on Different Traffic Load Patterns and Performance Metrics,” *Electronics*, vol. 13, no. 14, pp. 1-31, 2024. [CrossRef] [Google Scholar] [Publisher Link]

[10] S. Xu, and Tarek Saadawi, "Does the IEEE 802.11 MAC Protocol Work Well in Multihop Wireless Ad Hoc Networks?," *IEEE Communications Magazine*, vol. 39, no. 6, pp. 130-137, 2001. [CrossRef] [Google Scholar] [Publisher Link]

[11] Xia Li, Kee-chaing Chua, and Peng-yong Kong, "The Study of False Route Breakage in IEEE 802.11 based Ad Hoc Networks," *2006 IEEE International Conference on Mobile Ad Hoc and Sensor Systems*, Vancouver, BC, Canada, pp. 493-496, 2006. [CrossRef] [Google Scholar] [Publisher Link]

[12] Alvin Valera, Hwee-Pink Tan, and Winston K.G. Seah, "Improving Link Failure Detection and Response in IEEE 802.11 Wireless Ad Hoc Networks," *21st Annual IEEE International Symposium on Personal, Indoor and Mobile Radio Communications (PIMRC)*, Istanbul, Turkey, pp. 1814-1819, 2010. [CrossRef] [Google Scholar] [Publisher Link]

[13] Ratnesh Kumar Dubey et al., "Comparative Study of Load Analysis in MANET Routing Protocols: AODV vs. AOMDV," *2024 IEEE 4th International Conference on ICT in Business Industry and Government (ICTBIG)*, Indore, India, pp. 1-6, 2024. [CrossRef] [Google Scholar] [Publisher Link]

[14] Ibrahim Mohsen Selim et al., "MANET Routing Protocols' Performance Assessment Under Dynamic Network Conditions," *Applied Sciences*, vol. 15, no. 6, pp. 1-29, 2025. [CrossRef] [Google Scholar] [Publisher Link]

[15] Satveer Kour et al., "Evaluation of MANET Routing Protocols: Effects of Terrain Dimensions and Network Scalability," *Procedia Computer Science*, vol. 259, pp. 1479-1489, 2025. [CrossRef] [Google Scholar] [Publisher Link]

[16] Kevin Fall, and Kannan Varadhan, *The ns Manual (formerly ns Notes and Documentation)*, The VINT Project, UC Berkeley, LBL, USC/ISI and Xerox PARC, pp. 19-231, 2008. [Google Scholar]

[17] Ben Liang, and Zygmunt J. Haas, "Predictive Distance-based Mobility Management for PCS Networks," *IEEE INFOCOM '99. Conference on Computer Communications. Proceedings. Eighteenth Annual Joint Conference of the IEEE Computer and Communications Societies. The Future is Now (Cat. No.99CH36320)*, New York, USA, pp. 1377-1384, 1999. [CrossRef] [Google Scholar] [Publisher Link]

[18] Priyanka Pandey, and Raghuraj Singh, "Efficient Ad Hoc on Demand Distance Vector Routing Protocol based on Route Stability in MANETs," *International Journal of Wireless Information Networks*, vol. 29, no. 3, pp. 393-404, 2022. [CrossRef] [Google Scholar] [Publisher Link]

[19] Uppalapati Srilakshmi et al., "A Secure Optimization Routing Algorithm for Mobile Ad Hoc Networks," *IEEE Access*, vol. 10, pp. 14260-14269, 2022. [CrossRef] [Google Scholar] [Publisher Link]

[20] Ayoub Abdellaoui et al., "Enhancing Stability and Efficiency in Mobile Ad Hoc Networks (MANETs): A Multicriteria Algorithm for Optimal Multipoint Relay Selection," *Information*, vol. 15, no. 12, pp. 1-17, 2024. [CrossRef] [Google Scholar] [Publisher Link]

[21] P. Malarvizhi, and G. Kavithaa, "Identifying Stable Path in Self Configured Networks using Particle Swarm Optimization with Centrality Betweenness," *Journal of Electrical Engineering and Technology*, vol. 19, no. 4, pp. 2701-2713, 2024. [CrossRef] [Google Scholar] [Publisher Link]

[22] Swati B. Singh et al., "An Adaptive, Energy-Efficient and Secure Routing Protocol for Zone-Related Mobile Ad-Hoc Networks using Reinforcement Learning," *Scientific Reports*, vol. 16, no. 1, pp. 1-23, 2026. [CrossRef] [Google Scholar] [Publisher Link]

[23] Ako Muhammad Abdullah, "An Efficient Approach for Minimizing Control Packets and Enhancing Route Stability in Mobile Ad-Hoc Networks," *The Journal of Supercomputing*, vol. 82, no. 5, 2026. [CrossRef] [Google Scholar] [Publisher Link]

[24] Gavin Holland, and Nitin Vaidya, "Analysis of TCP Performance over Mobile Ad Hoc Networks," *Proceedings of the 5th Annual ACM/IEEE International Conference on Mobile Computing and Networking (MobiCom)*, Association for Computing Machinery, New York, United States, pp. 219-230, 1999. [CrossRef] [Google Scholar] [Publisher Link]

[25] Jinyang Li et al., "Capacity of Ad Hoc Wireless Networks," *Proceedings of the 7th Annual International Conference on Mobile Computing and Networking (MobiCom)*, Association for Computing Machinery, New York, United States, pp. 61-69, 2001. [CrossRef] [Google Scholar] [Publisher Link]